

The trigger for $K^0 \rightarrow \pi^0 \pi^0$ decays of the NA48 experiment at CERN

M. Cirilli

Scuola Normale Superiore e Sezione INFN di Pisa, I-56100 Pisa, Italy*
Manuela.Cirilli@cern.ch

Abstract

The trigger used for the collection of the samples of $K^0 \rightarrow \pi^0 \pi^0$ decays in the NA48 experiment at CERN uses a novel pipeline design in order to satisfy the demanding specifications of a high rate kaon beam. The trigger algorithms, architecture and performance are described.

I. INTRODUCTION

The NA48 experiment at CERN is designed to study direct CP violation by evaluating the real part of the parameter ε' . This is done by counting the number of K_L and K_S into $\pi^+ \pi^-$ and $\pi^0 \pi^0$ (where $\pi^0 \rightarrow \gamma \gamma$) decays to measure the double ratio

$$R = \frac{\Gamma(K_L^0 \rightarrow \pi^0 \pi^0) \Gamma(K_S^0 \rightarrow \pi^+ \pi^-)}{\Gamma(K_S^0 \rightarrow \pi^0 \pi^0) \Gamma(K_L^0 \rightarrow \pi^+ \pi^-)} \cong 1 - \Re\left(\frac{\varepsilon'}{\varepsilon}\right) \quad (1)$$

The measurement is actually performed by triggering on the four decay modes and counting the ones which pass the containment and background rejection cuts which are made offline. Systematic uncertainties due to changes in detector efficiencies are reduced by collecting the four decay channels simultaneously, while acceptance corrections are minimised by using almost collinear K_L and K_S beams and by weighting the K_L events to make the decay length distribution the same as that of the K_S events. The K_S and K_L decays are distinguished by tagging the protons which produce the K_S . The limiting mode for the statistics is the decay $K_L \rightarrow \pi^0 \pi^0$, which has a branching ratio of 9×10^{-4} . An overall sensitivity of 2×10^{-4} on $\Re(\varepsilon'/\varepsilon)$ has been reached in three years of data taking (1997-1999 and 2001), with the high intensity K_L beam delivering 500K decays per second [1].

This paper is concerned with the sub-system known as "the neutral trigger" [2], i.e. the sub-system responsible for triggering on K_L and K_S decays into $\pi^0 \pi^0$ final states. The main background to these signal events comes from $K_L \rightarrow 3\pi^0$ decays with overlapping or undetected photons. The $3\pi^0$ decays represent the dominant K_L decay channel, with a $\sim 21\%$ branching ratio. In spite of this very unfavourable signal to noise ratio, the trigger design was mainly driven by the need of a remarkably high efficiency rather than a high purity. The reason for this choice lies in the basic principle of the double ratio technique: in order to perform a precision measurement of $\Re(\varepsilon'/\varepsilon)$ with this technique, the unavoidable

systematic biases in the counting process must be symmetric between at least two of the four modes in the double ratio. The requirements this places on the neutral trigger system are:

- a very high efficiency (above $\sim 99\%$), which can be evaluated to better than one part per thousand; this is required to avoid large correction to $\Re(\varepsilon'/\varepsilon)$ due to different kinds of inefficiencies for $K_L \rightarrow \pi^0 \pi^0$ and $K_S \rightarrow \pi^0 \pi^0$;
- a low dead time, because any dead time condition on a decay mode must be applied to all the others decay modes to maintain the principle of simultaneous collection;
- a well understood response to decays which occur close in time to other activity (accidentals);
- a good rejection of the high rate of uninteresting decays;
- a fast delivery of trigger decisions.

The neutral trigger is thus designed as a fully synchronous pipelined system. It continuously performs computations on the digitised and summed information from the 13,248 channels of the electromagnetic calorimeter. It reconstructs online the energy of the kaon (with a 3% resolution), the decay position along the beam (to 3m over a distance of 100m), the number of photons and their arrival times (to 3ns). The proper decay time of the kaon is derived from the energy and decay position.

The trigger implements these calculations every 25ns in a dead-time-free pipeline, and performs a selection based on the reconstructed physical quantities. A weak transverse momentum cut is also applied. All these selection cuts are programmable, providing the possibility of setting trigger requirements for events other than the $K^0 \rightarrow \pi^0 \pi^0$ decays, like neutral kaon rare decays or $\eta \rightarrow \gamma \gamma$ decay. The neutral trigger also provides the total energy of the event by summing the energy from the hadron and the electromagnetic calorimeters. This is used to impose a total energy threshold on $K^0 \rightarrow \pi^0 \pi^0$ triggered events.

II. THE NEUTRAL PARTICLE DETECTORS

Kaons in the NA48 beams have an average energy of 110GeV and decay in flight. The decay products travel along the z direction for about 100m before reaching the detectors. Photons from $\pi^0 \pi^0$ decays are measured by the quasi-homogeneous LKr calorimeter: this is a liquid krypton

* Present address: Dipartimento di Fisica dell'Universit a di Roma "La Sapienza", I-00185 Roma, Italy .

ionization chamber, with a 127cm ($27X_0$) deep active region. The Molière radius of the showers is 4.7cm, which is somewhat larger than in sampling calorimeters. The read-out is arranged in a tower structure of copper ribbons defining the electrostatic cells. The cells are not strictly parallel, but widen slightly by 10mrad in order to point to the average position along the beam where the kaons in the accepted energy range decay.

There are a total of 13,248 cells arranged to define a cartesian grid of $2 \times 2 \text{cm}^2$ cells on which photons impact. The x and y axes, respectively, define the horizontal and vertical directions in the plane orthogonal to the beam line (see Fig.1). The sensitive area of the calorimeter forms an octagon, and can be considered a 128×128 cell square grid with the corners missing.

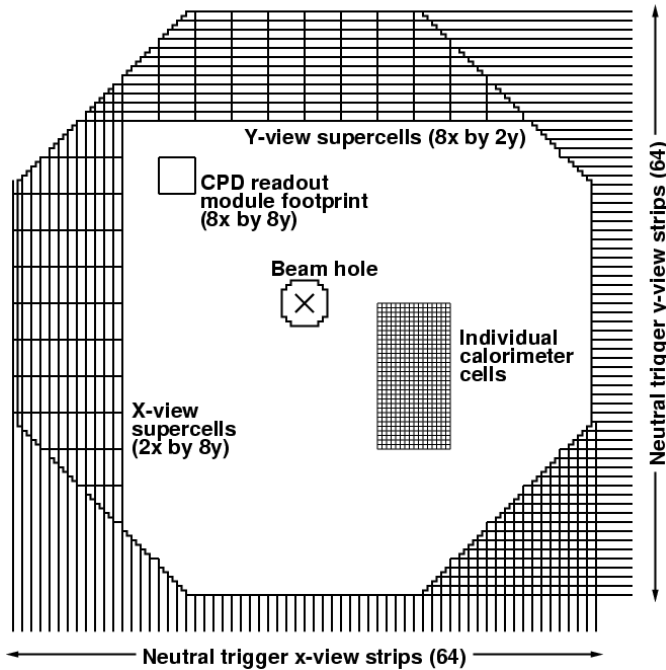


Figure 1. Front view schematic of the LKr calorimeter

The maximum drift distance within a cell is 1cm. The electrostatic field within the cells is 3kV/cm, and the corresponding electron drift velocity is 0.3cm/ μ s. The preamplifiers and switching circuits for the calibration system are mounted directly on the ends of the cells inside the liquid krypton. The signals go through further amplification and shaping stages at the feedthroughs of the krypton cryostat and on the CPD readout modules.

The shaping circuits differentiate the signals so that only the fast initial rise of the current produces the pulse which is used in the neutral trigger and in the readout. This arrangement results in a fast detector (the signal pulse has a FWHM of ~ 70 ns) with good energy, position and time resolution. A 3% flat undershoot on the signal is present for the $\sim 3 \mu$ s following each pulse during which electrons continue to drift across the electrode gap. At 25GeV, the energy resolution is better than 1%, the spatial resolution is 1mm and the time resolution of a single shower is 280ps.

The neutral hodoscope consists of bundles of scintillating fibres placed vertically within the liquid krypton calorimeter at a depth of $\sim 9.5X_0$, corresponding to the maximum development depth of an average electromagnetic shower. The scintillators are read out with photomultiplier tubes. The neutral hodoscope is used to generate an independent and unbiased trigger on neutral decays; this trigger is generated by the coincidence of two hits in two half-planes of the hodoscope, either horizontally (left and right) or vertically (top and bottom), and runs at about 30kHz. Neutral hodoscope (NHOD) triggers are downscaled by a factor 100 and collected in order to measure the $\pi^0\pi^0$ trigger efficiency.

III. THE NEUTRAL TRIGGER

A. Overview

The NA48 neutral trigger design has to satisfy the requirements already stated in section I, which are dictated by the experimental technique adopted to measure ϵ' . In addition, the trigger has to cope with the high rate of particles in the detector, which is of the order of 500kHz. All these considerations led to the exclusion of the "classic" trigger design with several levels of filtering, realized with different technologies, and to the choice of implementing the system as a single 128-steps synchronous pipeline running at the common experiment clock frequency of 40-MHz. This design extends the complexity of what is the classical first-level trigger, and removes completely the second-level trigger.

In this scheme, raw-data from the calorimeter is continuously flash-digitised and stored in a 200 μ s buffer, while the neutral trigger performs the complete event reconstruction for each 25ns time interval irrespective of whether there was any physics-related activity in the detector. The various additions, conversions, multiplications etc. are performed by dedicated circuitry and the data is transformed into the trigger decision as it traverses the pipeline. The trigger decision is delivered synchronously with the detector signals, 25ns \times 128 = 3.2 μ s after the first pipeline step. Although the circuitry is never idle, it spends a large fraction of its time computing the case when there was no detector activity. This approach has the advantages that there is no dead time (the pipeline never has to wait for a preceding event), there are no limitations due to complex event topologies and the system is simple and stable to operate. The beams are debunched before being extracted from the SPS accelerator so that the time distribution of kaon decays is roughly uniform within the 2.4s machine spill.

Whenever an event satisfies the neutral trigger cuts, the system identifies the time-slice at which the event occurred and generates a trigger relative to that time. The trigger decision is sent to the trigger supervisor system which records the absolute event time.

B. Trigger Algorithms

Whenever a kaon disintegrates into n massless particles (photons) which impact on the calorimeter, the total energy E ,

centre of gravity C and vertex decay position D as measured by the LKr are given by:

$$E = \sum_{p=1}^n E_p \quad (2)$$

$$C^2 = \frac{1}{E^2} \left(\sum_{p=1}^n E_p x_p \right)^2 + \frac{1}{E^2} \left(\sum_{p=1}^n E_p y_p \right)^2 \quad (3)$$

$$D^2 = \frac{1}{m_K^2} \sum_{p=1}^n \sum_{q \neq p}^n E_p E_q d_{pq}^2, \quad (4)$$

where E_p , x_p and y_p are the energies and impact positions of the photons in the calorimeter, m_K is the mass of the kaon, and d_{pq} is the distance between the impact positions of photons p and q . The centre of gravity represents the point where the kaon would hit the front face of the calorimeter, if it had not decayed before. This virtual impact point is an estimate of the kaon's transverse momentum.

The above expressions can be reformulated in terms of the total energy from the photons and of the impact positions on calorimeter strips oriented along the two axes x and y of the cartesian grid formed by the read-out cells. Let $E_i^{(x)}$ and $E_i^{(y)}$ denote the energy on the i th strip in the x and y projections respectively; E , C and D are then given by

$$E = \sum_i E_i^{(x)} = \sum_i E_i^{(y)} \quad (5)$$

$$C^2 = \frac{x_0^2}{E^2} \left(\sum_i E_i^{(x)} i \right)^2 + \frac{y_0^2}{E^2} \left(\sum_i E_i^{(y)} i \right)^2 \quad (6)$$

$$D^2 = \frac{1}{m_K^2} \left(E x_0^2 \sum_i E_i^{(x)} i^2 + E y_0^2 \sum_i E_i^{(y)} i^2 - E^2 C^2 \right), \quad (7)$$

where x_0 and y_0 denote the strip widths in the x and y projections. The importance of this rearrangement is that it allows these quantities to be reconstructed without a pattern recognition step to identify the photons. Indeed, the expressions are independent of the number of photons into which the kaon disintegrated. Eq. (7) gives an approximate expression of the vertex decay position, because the energy of the photon is spread over several adjacent strips instead of being concentrated at the photon impact position. The approximation is evident in the case of an event consisting of a single photon, for which D is zero in Eq. (4) whereas it is slightly positive in Eq. (7).

These quantities are then used to compute the proper decay time in units of the K_S lifetime τ_S

$$\frac{\tau}{\tau_S} = \frac{m_K c^2 (z_0 - D)}{E c \tau_S}$$

where c is the speed of light and z_0 is the distance between the beginning of the decay fiducial volume (where $\tau \sim 0$) and the front face of the calorimeter (where impact positions are defined).

Eqs. (5)-(7) summarise the actual way in which the trigger computation proceeds. The strips in each projection are built up from 'supercells' of 2x8 cells each (see Fig.1). The

summation of the energies in the sixteen gain-equalised cells in each supercell is performed using analogue summing circuits; the supercell pulse is then digitised at the pipeline frequency of 40MHz using 10-bit flash ADCs (2000 channels in total) and the output is filtered to exclude baseline and noise effects.

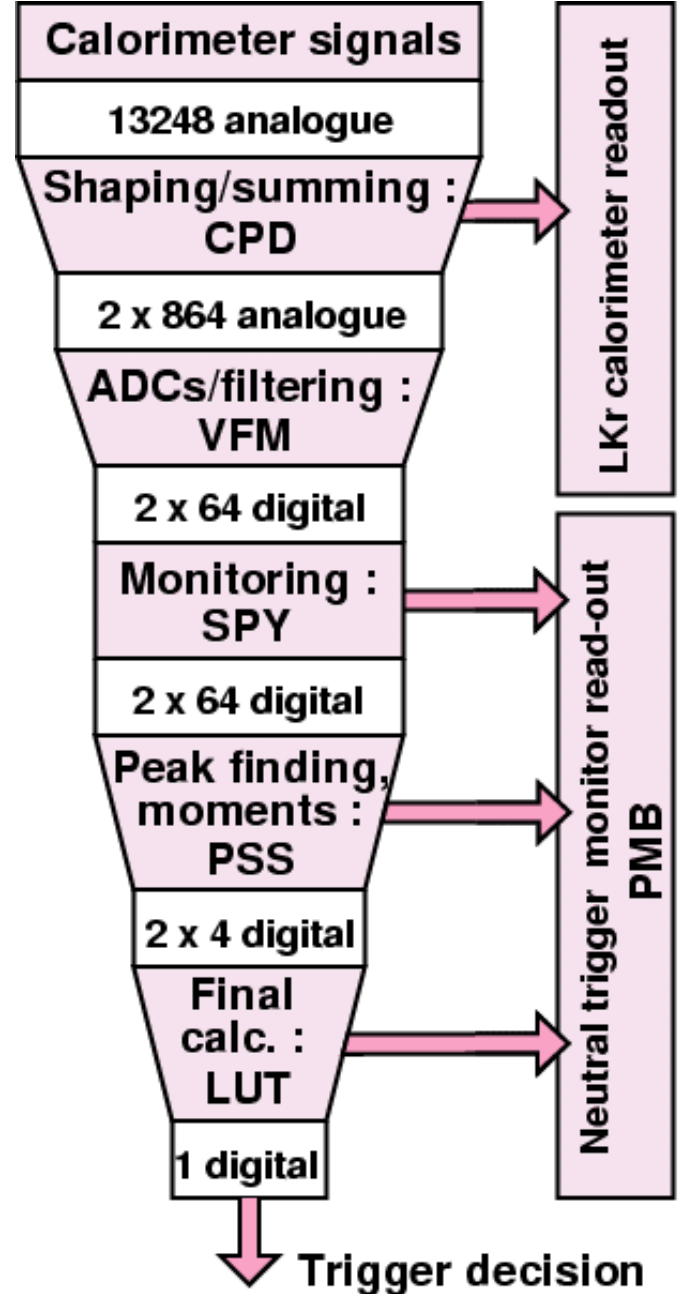


Figure 2 Overview of the Neutral Trigger electronics chain

The summation of the 16 supercells to build one strip is performed digitally. The digitisation, filtering and digital summations are performed in the Filter Module system (VFM), while signal shaping, gain equalisation and analogue summation are done on the Calorimeter Pipeline Digitiser modules (CPD) which also house the calorimeter readout. The x and y projections of the calorimeter are then used to

compute the above quantities in the pipeline. The projection information is also used to perform peak finding and to find out the arrival time of each peak. The construction of each sum in equations (5)-(7) and the peak finding are performed in the PeakSum system (PSS) and the final computations and trigger cuts are performed in the look-up table modules (LUT). A schematic of the complete trigger pipeline chain is shown in Fig.2.

IV. PERFORMANCE

The neutral trigger system has successfully operated since the first NA48 physics run in 1997. The online trigger cuts are summarised in Table 1, along with the corresponding selections applied in the offline analysis. The peak cut is implemented by summing up the number of peaks within a 9.375ns wide time window. The cut requiring less than 6 peaks is not applied when there are peaks surrounding this time window, since this is evidence that the event was accompanied by other (accidental) clusters not associated with the triggered event.

Cut	Trigger	Offline
Energy	>50 GeV	>70 GeV
Centre of gravity	<15 cm	<10 cm
Lifetime	< 5 τ_s	< 3.5 τ_s
x projection peaks	< 6 peaks within 3x3.125 ns	4 photons
y projection peaks	< 6 peaks within 3x3.125 ns	4 photons

Table 1 Summary of the variables computed online by the Neutral Trigger, along with their cut values and the corresponding offline cuts.

The rate of particles in the detector is ~ 500 KHz, and the output rate of the neutral trigger is ~ 2 KHz. The number of $\pi^0\pi^0$ triggers collected in each burst is of the order of 5,000; about 30 of these events satisfy the full offline $\pi^0\pi^0$ selection criteria.

Trigger performance studies are done by analysing the data received by the PMB monitoring system. Information collected by the PMBs, or "trigger variables", are compared with the "offline variables", reconstructed using the data collected by the main read-out system. Downscaled events triggered by the neutral hodoscope are collected during ϵ' data taking. These NHOD triggers provide a sample of unbiased events for neutral trigger efficiency studies.

The neutral trigger energy resolution for single photon detection is checked performing the ratio between offline and trigger cluster energies in bins of 5 GeV. The mean and the sigma of the distribution in each bin are then obtained from a gaussian fit. The neutral trigger underestimates the energy in the case of low energy photons, while high energy clusters are overestimated. This non-linearity is mainly caused by the energy dependence of the lateral shower leakage into supercells which are below threshold in the VFMs. The

neutral trigger has an energy resolution of about 3% in the high energy range.

Concerning the calculation of the lifetime, the neutral trigger underestimates τ by about $0.5\tau_s$ on average: this is mainly due to a small left-over offset in the energy scale calibration, which ensures high efficiency on all events. The vertex position needed to compute the proper decay time is reconstructed with an accuracy of around 3m over a distance of 100m.

A crucial feature of the neutral trigger system is the online evaluation of clusters' times performed by the PeakSum system. This is essential to reduce the amount of accepted $K_L \rightarrow 3\pi^0$ decays while avoiding large inefficiencies due to accidental activity in the detector. Clusters are considered as coincident when they fall within a ~ 10 ns time window (see Table 1). The width of the time window is chosen on the basis of the time resolution that the system can achieve: the better the PeakSum system is able to reconstruct the cluster times, the smaller the coincidence window can be defined. A small time window reduces the losses due to accidental decays superimposed to the 4 photons of a $K^0 \rightarrow \pi^0\pi^0$ event.

The PeakSum resolution is better than 2.5ns in both views. This is an excellent performance, since this resolution is obtained with no geometrical selection criteria on the photon impact positions and thus is affected by the effects of possible skews between different calorimeter channels.

The neutral trigger efficiency is evaluated using the control sample of events triggered by the neutral hodoscope which survive the full offline $\pi^0\pi^0$ selection. Events are defined as inefficient if the neutral trigger bit is not present in a window of ± 2 time-slices around the triggered event.

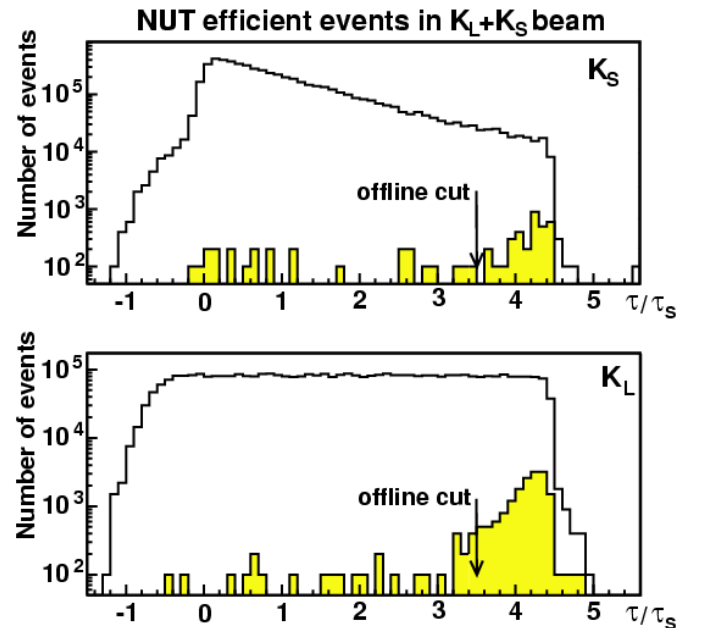


Figure 3 Distributions of NHOD events

Fig. 3 shows how NHOD events are distributed as a function of the proper decay time in units of τ_s ; inefficient events are also shown on the same plot. The events have been

identified as K_S or K_L decays using the tagging detector, which tags the proton hitting the K_S target. The K_S distribution contains a contamination of $\sim 10.6\%$ of the true K_L events (mistagging).

The cut on τ/τ_S applied by the neutral trigger is set to provide high efficiency for events with $\tau/\tau_S < 3.5$ which are accepted in the ε' offline analysis. In addition, K_L events are weighted according to the K_S lifetime distribution, in order to have the same decay spectra for both beams.

During the 1997 run, the LKr calorimeter operated at half the nominal 3kV drift voltage, and a 4cm column in the x projection was without high voltage (due to a failure in the HV connection). The neutral trigger demonstrated its flexibility in this difficult experimental situation: a flag in the VFMs was set for this whole column and the number-of-peaks cut in the x view was loosened to ≤ 6 peaks. The trigger efficiency for $\pi^0\pi^0$ decays during the 1997 run was $(99.88 \pm 0.04)\%$, with no differences between K_L and K_S .

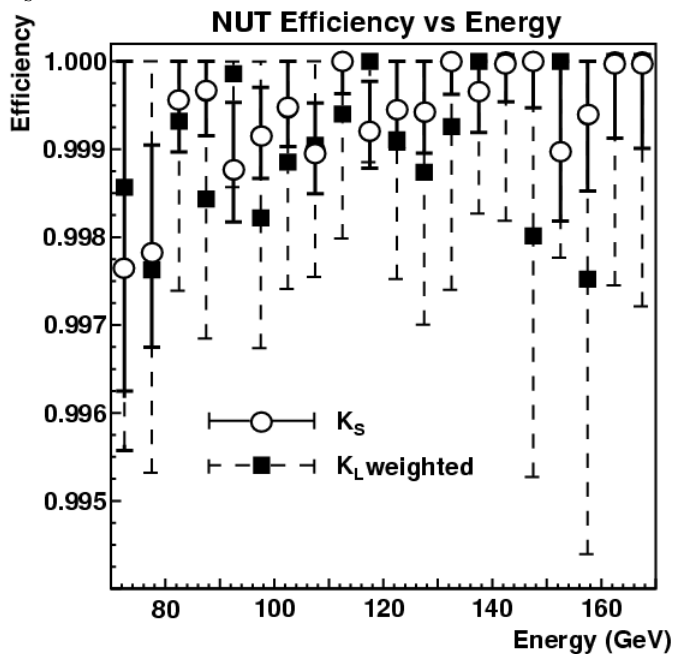


Figure 4 Trigger efficiency as a function of the kaon energy

Since 1998, the high voltage of the calorimeter has been set at 3kV and beam intensities have been increased. The overall neutral trigger efficiency during the 1998 and 1999

data taking was $(99.920 \pm 0.009)\%$, and was the same for K_L and K_S events: this fact is of utmost importance for the ε' measurement, since it implies that no correction has to be applied to the double ratio to correct for biases in the neutral trigger behaviour. The trigger efficiency for these two run periods is plotted in Fig. 4 as a function of the kaon energy, for K_S and weighted K_L decays

Event losses have been studied by looking at the trigger and offline information recorded along with each inefficient event. The main source of inefficiencies is the occurrence of two distinct classes of accidental decays, namely:

- High energy Λ baryons decaying far upstream in the K_L beam-line within ~ 40 ns of the good event. The energy deposited by the isolated protons from these decays shifts the centre of gravity reconstructed by the trigger towards higher values, so that the event fails the 15cm trigger cut on this quantity.
- Accidental $K_L \rightarrow 3\pi^0$ decay occurring within 10ns of the good event. This causes a higher number of reconstructed peaks in the trigger with respect to the cut value.

Another cause of inefficiency is an occasional energy mismeasurement due to the bad response or mis-calibration of a cell.

V. CONCLUSIONS

The neutral trigger for the NA48 experiment has successfully operated over several years. The novelty of this system is largely its architecture, where the entire trigger computation is performed in a single continuously running pipeline. This approach has proven very successful: trigger operation is convenient and stable, with no unforeseen difficulties during set-up since a sufficient amount of hardware diagnostic circuitry had been implemented. The trigger efficiency was carefully studied and is well understood.

VI. REFERENCES

- [1] A. Lai et al, Eur. Phys. Jour. C22 (2001) 231
- [2] G.Barr et al, Nucl. Instr. and Meth. A 485(2002) 676